

Mechanisms Underlying the Dual-Mode Regulation of Microtubule Dynamics by Kip3/Kinesin-8

Xiaolei Su,^{1,2,3,4} Weihong Qiu,⁴ Mohan L. Gupta, Jr.,⁵ José B. Pereira-Leal,⁶ Samara L. Reck-Peterson,⁴ and David Pellman^{1,2,3,4,*}

¹Howard Hughes Medical Institute

²Department of Pediatric Oncology, Dana-Farber Cancer Institute

³Department of Pediatric Hematology/Oncology, Children's Hospital

⁴Department of Cell Biology

Harvard Medical School, Boston, MA 02115, USA

⁵Department of Molecular Genetics and Cell Biology, University of Chicago, Chicago, IL 60637, USA

⁶Instituto Gulbenkian de Ciência, P-2781-901 Oeiras, Portugal

*Correspondence: david_pellman@dfci.harvard.edu

DOI 10.1016/j.molcel.2011.06.027

SUMMARY

The kinesin-8 family of microtubule motors plays a critical role in microtubule length control in cells. These motors have complex effects on microtubule dynamics: they destabilize growing microtubules yet stabilize shrinking microtubules. The budding yeast kinesin-8, Kip3, accumulates on plus ends of growing but not shrinking microtubules. Here we identify an essential role of the tail domain of Kip3 in mediating both its destabilizing and its stabilizing activities. The Kip3 tail promotes Kip3's accumulation at the plus ends and facilitates the destabilizing effect of Kip3. However, the Kip3 tail also inhibits microtubule shrinkage and is required for promoting microtubule rescue by Kip3. These effects of the tail domain are likely to be mediated by the tubulin- and microtubule-binding activities that we describe. We propose a concentration-dependent model for the coordination of the destabilizing and stabilizing activities of Kip3 and discuss its relevance to cellular microtubule organization.

INTRODUCTION

Microtubules are filamentous polymers that are assembled from α/β -tubulin heterodimers. Individual microtubules alternate between growth and shrinkage, a phenomenon known as dynamic instability (Mitchison and Kirschner, 1984). Microtubule dynamic instability enables rapid remodeling of the microtubule cytoskeleton that is essential for diverse cellular processes such as cell division, cell migration, and axon outgrowth (Poulain and Sobel, 2010; Walczak and Heald, 2008; Wehrle-Haller and Imhof, 2003).

Cellular microtubules are polarized, having a more dynamic plus end and a less dynamic minus end. The regulation of the microtubule plus end is particularly important because many

critical dynamic interactions occur at the plus end: for example, interactions with attachment sites on the cell cortex and the kinetochore. The growing plus end is structurally and chemically distinct from the lattice: whereas the microtubule lattice is composed of GDP-liganded β -tubulin, the growing plus end has a GTP cap, with GTP- β -tubulin. The GTP cap is thought to stabilize the plus ends of growing microtubules. Loss of the GTP cap, coupled with structural changes at the plus end, results in "catastrophe" (the transition from growing to shrinking). Shrinking microtubules can also make transitions to growth, which is termed as "rescue" (Desai and Mitchison, 1997; Howard and Hyman, 2009).

Many key microtubule regulators accumulate at the microtubule plus end. In live cell imaging experiments, these proteins, called microtubule plus end tracking proteins or +TIPs, give the appearance of "surfing" on the microtubule plus end (Carvalho et al., 2003; Schroer, 2001; Schuyler and Pellman, 2001). +TIPs use different strategies to associate with plus ends: binding plus end-specific structures (that have yet to be clearly defined), being retained at the plus end after reaching it by diffusion or directional translocation, or "hitchhiking" on other +TIPs (Galjart, 2010).

Despite the plethora of proteins at the microtubule plus end, there are a few highly conserved factors that appear to be the critical plus end regulators: EB family proteins in general promote plus end dynamics and serve as platforms for recruiting many other proteins to the plus end. XMAP215/Dis1 family proteins accelerate microtubule growth, and the nonmotile kinesin-13s are major cellular catastrophe-promoting factors (Akhmanova and Steinmetz, 2008; Gouveia and Akhmanova, 2010). Recently motors of the kinesin-8 family have been the focus of much investigation because they have an evolutionarily conserved role in governing global cellular microtubule lengths. However, the mechanism by which they control microtubule plus end dynamics is complex and less well understood than the other critical plus end regulators.

The kinesin-8 family of motors are found throughout eukaryotes (Wickstead and Gull, 2006), and there is a strong functional conservation across species. The loss of kinesin-8s in cells generally results in long microtubules, which will affect many

cellular processes. Loss of the budding yeast kinesin-8, Kip3, causes defects in spindle positioning, kinetochore clustering, and spindle disassembly (DeZwaan et al., 1997; Straight et al., 1998; Wargacki et al., 2010). In fission yeast, *klp5* and *klp6* are involved in chromosome alignment and are essential for meiosis (West et al., 2002; West et al., 2001). Kinesin-8s in higher eukaryotes (*Drosophila* and mammals) are essential for progression through mitosis and are required for chromosome congression (Gandhi et al., 2004; Stumpff et al., 2008). These cellular functions of kinesin-8s can be largely attributed to their complex effects on regulating microtubule dynamics. Consistent with their requirement to limit microtubule length, kinesin-8s promote catastrophe in a microtubule length-dependent manner (Tischer et al., 2009) and slow the rate of microtubule growth (Du et al., 2010). However, kinesin-8s also have apparent stabilizing effects on microtubules. In both budding yeast and human cells, kinesin-8s slow the microtubule shrinkage rate and also increase the frequency of rescue (Du et al., 2010; Gupta et al., 2006). The combination of promoting length-dependent catastrophe and stabilizing shrinking microtubules enables kinesin-8s to narrow down the length variation of microtubules, for example, during metaphase chromosome alignment (Stumpff et al., 2008).

The mechanisms by which kinesin-8s regulate microtubule dynamics are only just starting to be understood. All kinesin-8s investigated are plus end-directed microtubule motors. The budding yeast kinesin-8, Kip3, also has plus end-specific depolymerase activity, manifested as the ability to depolymerize GMPCPP-stabilized microtubules (Gupta et al., 2006; Varga et al., 2006). GMPCPP is a slow-hydrolysable GTP analog, and therefore GMPCPP-stabilized microtubules are thought to structurally mimic the GTP cap on growing microtubule plus ends. The depolymerase activity of Kip3 may explain the catastrophe-promoting effect of Kip3 in cells. Kip3 is highly processive, and its depolymerase activity involves cooperative interactions among Kip3 motors (Varga et al., 2009). This results in preferential destabilization of longer microtubules over shorter ones. However, whether a similar depolymerase activity is the basis for the destabilizing effect *in vivo* for all kinesin-8s has been a subject of much debate (Du et al., 2010; Grissom et al., 2009; Mayr et al., 2007).

By contrast with the destabilizing/depolymerizing activities of kinesin-8s, the mechanistic basis for the stabilizing effects of kinesin-8s on microtubules has not been experimentally explored. There has been speculation that Kip3 might interact differently with the straight GTP-liganded tubulin on growing ends than it does with the bent GDP-liganded tubulin on shrinking ends (Gardner et al., 2008). We previously demonstrated that Kip3 accumulates on the plus ends of growing microtubules, when it destabilizes microtubules. The accumulation of Kip3 is lost on the plus ends of shrinking microtubules when a stabilizing effect was observed (Gupta et al., 2006). The basis for the stabilizing effect, as well as how the destabilizing and stabilizing effects of Kip3/kinesin-8 on microtubules are coordinated, is not understood.

Here we report that the tail domain of Kip3 is critical for both the destabilizing and stabilizing effects of Kip3 on microtubule dynamics. The Kip3 tail promotes the binding of Kip3 to growing or stabilized plus ends. It facilitates the depolymerase activity of

Kip3 and is essential for the destabilizing effect of Kip3 *in vivo*. However, on its own or in the context of a fusion to the nondepolymerizing kinesin-1, the Kip3 tail stabilizes microtubules. Furthermore, a Kip3 truncation lacking the tail domain is deficient for stabilizing shrinking microtubules. The effects of the Kip3 tail on microtubule dynamics may be mediated by a tubulin-binding activity that we report in this study. Together, our findings provide mechanistic insights into the complex microtubule regulatory functions of kinesin-8s.

RESULTS

Construction of a Motility-Competent “Tail-less” Kip3

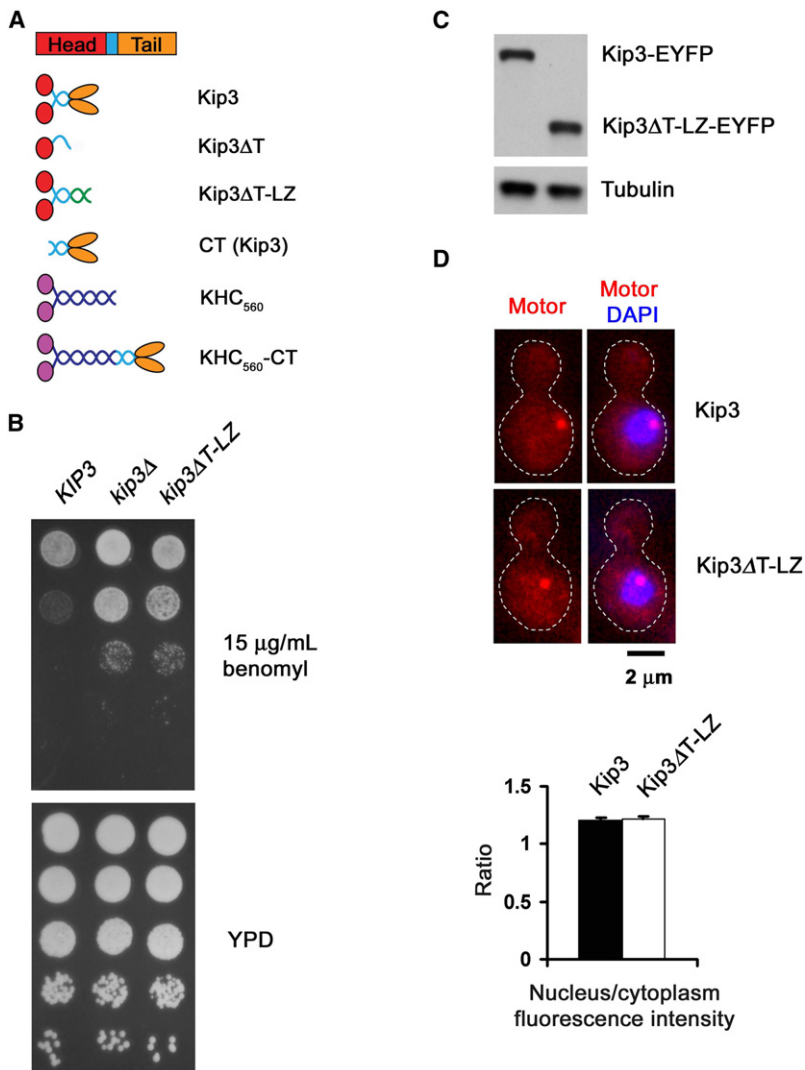
The N-terminal motor domains of kinesin-8s are conserved across species, whereas the C-terminal tail domains are more divergent. Budding yeast Kip3 has a robust depolymerase activity, which has not been detected for kinesin-8s from other organisms. We therefore asked whether the tail domain of Kip3 (amino acids 481–805) is important for promoting Kip3's depolymerase activity. A “tail-less” truncation construct (Figure 1A) was generated and expressed in yeast, and the truncated protein Kip3 Δ T was purified. This construct contained an N-terminal polyhistidine tag for purification followed by a Halo tag (Promega), which enables a 1:1 stoichiometric labeling of proteins with photostable fluorophores.

Our initial characterization of Kip3 Δ T revealed that the tail-less construct lacked motility because of a defect in dimerization. Ethylene glycol-bis (succinic acid N-hydroxysuccinimide ester) (EGS) crosslinking suggested that Kip3 Δ T was monomeric (see Figure S1A available online). Using total internal reflection microscopy (TIRF) we did not detect directional movement of tetramethylrhodamine (TMR)-labeled Kip3 Δ T; Kip3 Δ T made apparently diffusive excursions (Figure S1B). To create a motility-competent version of Kip3 Δ T, we introduced a leucine zipper motif (LZ) at the C terminus in a manner that maintained the register of the heptad repeats. EGS crosslinking demonstrated that this construct, Kip3 Δ T-LZ, was dimeric (Figure S1A). Kip3 Δ T-LZ exhibited directional and processive movement along microtubules (Figure S1B) that was comparable to that of full-length Kip3 previously described (Varga et al., 2006).

A Critical Role for the Kip3 Tail in Destabilizing Microtubules *In Vivo*

The generation of a motility-competent Kip3 tail truncation enabled us to determine if the tail domain of Kip3 contributes to the regulatory function of Kip3 on microtubule stability. A yeast strain was generated in which the *KIP3* open reading frame was replaced with a sequence encoding Kip3 Δ T-LZ under the control of the endogenous *KIP3* promoter. Cells lacking Kip3 are resistant to the microtubule-destabilizing drug benomyl, presumably due to the absence of the microtubule-destabilizing activity of Kip3. Strikingly, cells expressing Kip3 Δ T exhibited benomyl resistance to a degree similar to that of cells completely lacking Kip3 (Figure 1B). This led us to hypothesize that the Kip3 tail is critical for the destabilizing activity of Kip3.

Several control experiments further support the hypothesis that the Kip3 tail is directly involved in Kip3's regulation of



microtubule stability. First, the steady-state concentration of Kip3ΔT-LZ was indistinguishable from Kip3 (Figure 1C). Second, unlike fission yeast homologs, the Kip3 tail is not essential for normal nuclear import. We measured the relative amounts of EYFP-tagged Kip3 and Kip3 ΔT-LZ in the nucleus and in the cytoplasm (Figure 1D). This was done in mitotic cells where the microtubule-bound pool of the motors was eliminated by depolymerizing microtubules with nocodazole. Kip3 and Kip3 ΔT-LZ were similarly distributed between nuclear and cytoplasmic pools, suggesting the Kip3 tail is not required for nuclear localization of Kip3. This is likely explained by the fact that Kip3 is predicted by PSORT (<http://psort.hgc.jp/>) (Nakai and Horton, 1999) to contain nuclear localization sequences in both the motor and tail domains.

Next, we characterized the requirement of the tail domain for the mitotic functions of Kip3. In common with cells lacking Kip3, but in contrast to wild-type cells, cells expressing Kip3 ΔT-LZ exhibited declustered kinetochores in preanaphase cells (Figures 2A and 2B). This defect in kinetochore congression per-

Figure 1. The Kip3 Tail Is Critical for the Kip3-Mediated Regulation of Microtubule Stability In Vivo

(A) Schematic of the constructs used in this study. Kip3 contains an N-terminal motor domain (Head, red), followed by a short coiled-coil domain (blue) and a C-terminal tail domain (orange).

(B) Comparable benomyl resistance of *kip3ΔT-LZ* and *kip3Δ* stains relative to the *KIP3* control strains. Shown are 10-fold dilutions of cells from top to bottom spotted onto plates. (Top) Benomyl-containing plate. (Bottom) Control YPD plate.

(C) Similar steady-state protein levels of Kip3 and Kip3ΔT-LZ expressed from the endogenous *KIP3* promoter. Kip3/Kip3ΔT-LZ contains an EYFP tag and was detected with an anti-GFP antibody. Tubulin serves as a loading control.

(D) Deletion of the Kip3 tail does not alter its distribution between the nucleus and the cytoplasm. (Top) Single focal plane, wide-field images of Kip3-EYFP- or Kip3ΔT-LZ-EYFP (red)-expressing cells costained with DAPI (blue). Microtubules were depolymerized by treatment of cells with 35 μg/mL nocodazole for 15 min. The bright EYFP dot is the motor associated with spindle pole bodies or kinetochores. Cell boundaries are outlined by dashed white lines. (Bottom) Quantification of the ratio of nuclear to cytoplasmic fluorescence intensity of Kip3-EYFP and Kip3ΔT-LZ-EYFP. Preanaphase and anaphase cells were scored for the analysis. The data were represented as mean ± SEM (n = 75).

sisted until early anaphase, resulting in ~60% of cells with lagging chromosomes (Figures 2A and 2C). However, this defect was largely resolved by late anaphase/telophase. Lagging chromosomes in Kip3 ΔT-LZ-expressing cells were only slightly less prevalent in comparison to cells completely lacking Kip3. Also like *kip3* null cells, *kip3ΔT-LZ* cells have a defect in spindle disassembly, manifested as abnormally elongated anaphase/telophase spindles (Figures 2A and 2D). Taken together, our data

suggest a critical role of the Kip3 tail in regulating cellular microtubule stability.

The Kip3 Tail Contributes to Microtubule Plus End Binding and Depolymerase Activity of Kip3 In Vitro

Kip3 is a plus end-specific microtubule depolymerase. Microtubule depolymerization by Kip3 thus requires the following steps: the initial binding to microtubules, the processive movement of the motor along the body of the microtubule to the plus end, the accumulation at the plus end, and the initiation of microtubule depolymerization. To determine the molecular basis for the functional defects of Kip3 ΔT-LZ, we used single molecule imaging to systematically and quantitatively compare Kip3 ΔT-LZ with Kip3 for each step necessary for microtubule depolymerization (Figures 3A and 3B).

Most parameters were similar for the full-length motor and the tail-less construct: the on rates for productive interactions with microtubules (those that led to directional motility) were nearly identical, as were the motor velocities. However, Kip3 ΔT-LZ

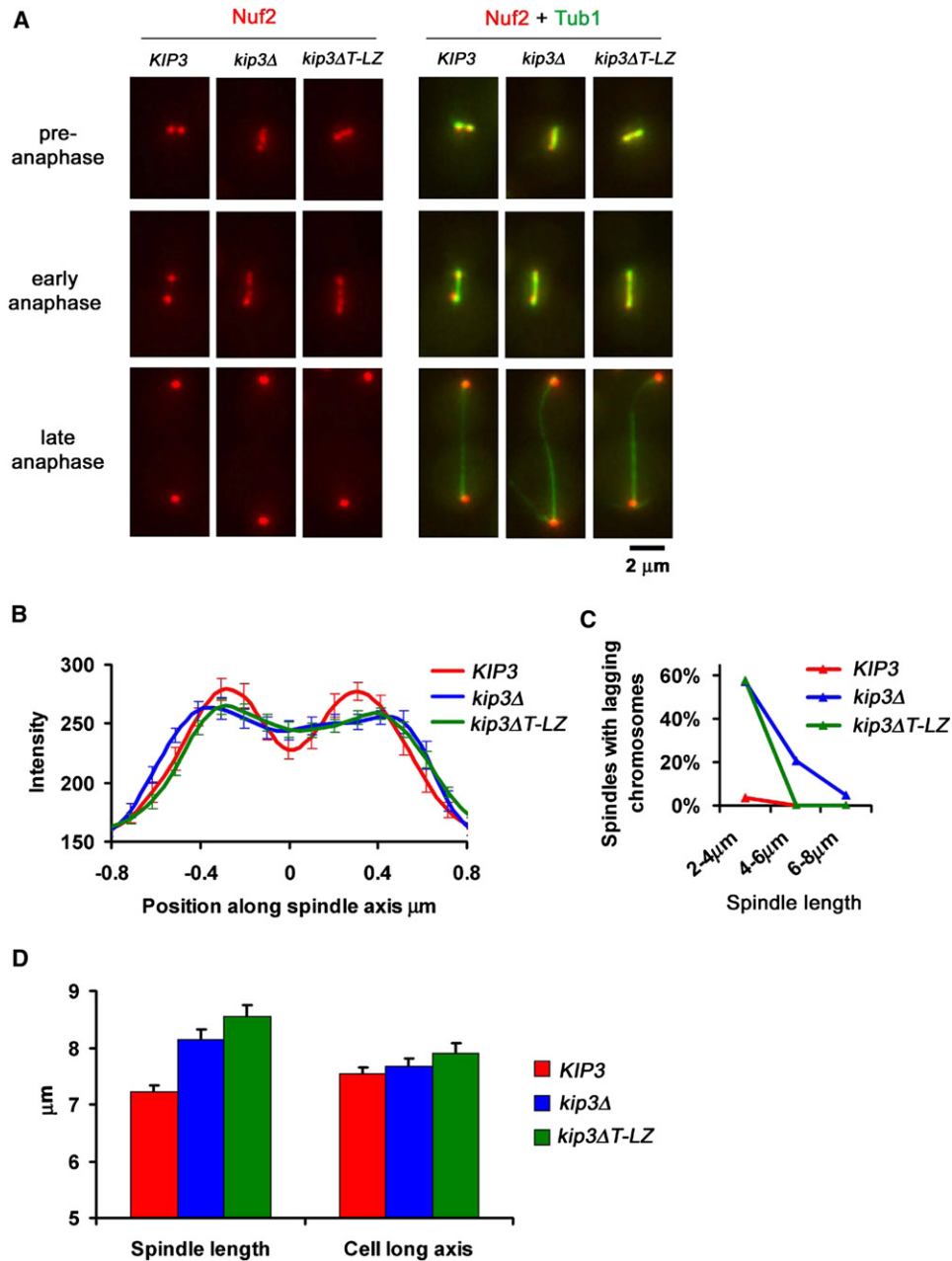


Figure 2. The Kip3 Tail Is Required for Normal Kinetochores Clustering and Spindle Disassembly during Cell Division

(A) Declustered kinetochores in *Kip3ΔT-LZ*-expressing cells. Kinetochores are labeled with Nuf2-GFP (red). Microtubules are labeled with CFP-Tub1 (green). Images of Nuf2 were acquired with a YFP filter set to eliminate cross-channel spillover.

(B) Line scans of Nuf2-GFP fluorescence intensity along preanaphase spindles in the indicated strains. Note that Nuf2 concentrates near the two spindle poles in *KIP3* cells but is loosely scattered along the spindle in *kip3Δ* and *kip3ΔT-LZ* cells. Each data point is presented as mean ± SEM (n = 15) and is connected by lines to assist visualization.

(C) Quantification of spindles with anaphase-lagging chromosomes. N = 131, 145, and 142 for *KIP3*, *kip3Δ*, and *kip3ΔT-LZ* cells, respectively.

(D) Defective spindle disassembly in *kip3ΔT-LZ* cells, detected as a longer anaphase spindle length prior to spindle breakdown. Time-lapse imaging was adopted to define the maximal spindle length prior to mitotic exit in cells containing CFP-Tub1. The comparable lengths of cell long axis indicate the cell sizes are not significantly different among the three strains. Each data point is presented as mean ± SEM (n = 15). The spindle lengths of *KIP3* and *kip3ΔT-LZ* cells prior to spindle breakdown are significantly different by t test (p < 0.00001).

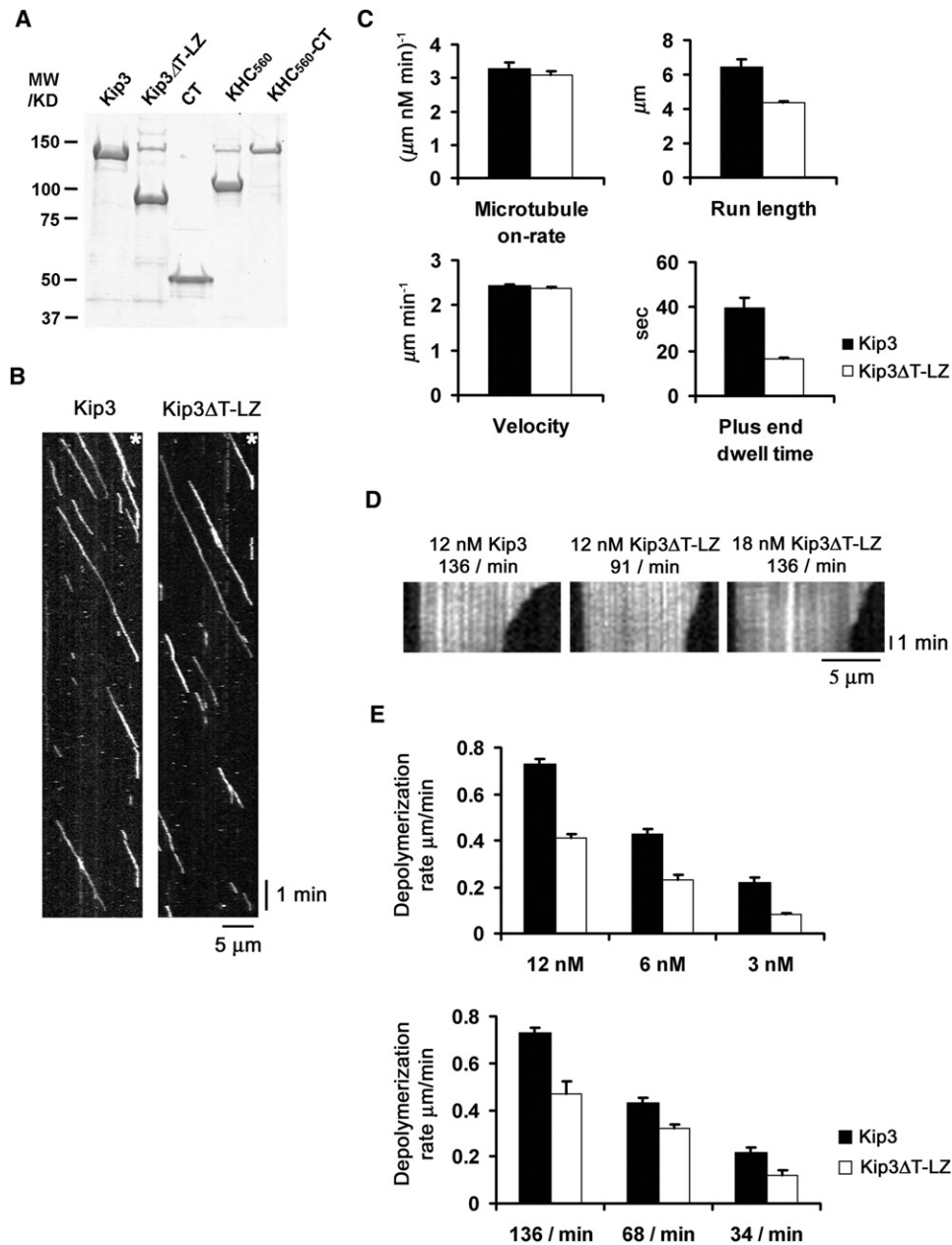


Figure 3. The Kip3 Tail Is Required for Efficient Microtubule Plus End Binding and Microtubule Depolymerase Activity In Vitro

(A) Coomassie blue-stained gel with the indicated proteins after purification.

(B) Kymographs from single molecule imaging experiment visualizing the motility of TMR-labeled Kip3 and Kip3ΔT-LZ on Taxol-stabilized microtubules by TIRF microscopy. An image of fluorescein-labeled microtubules was acquired separately to determine the position of microtubule ends, as indicated by white asterisks.

(C) Comparison of the microtubule on-rate, run length, velocity, and plus end dwell time between Kip3 and Kip3ΔT-LZ. The microtubule effective on-rate was defined as the number of processive translocation events ($>0.5 \mu\text{m}$ in run length) observed per minute divided by the length of each microtubule and the motor input concentration. The on-rate for 13 microtubules in each group was averaged. The velocity was fit to a Gaussian curve. The run length and dwell time at the plus ends were fit to a first-order exponential curve. The bar graphs show mean \pm SEM. Histograms of velocity, run length, and dwell time are shown in Figure S2.

(D) Depolymerization of microtubules by Kip3 and Kip3ΔT-LZ. Kymographs show depolymerization of GMPCPP-stabilized fluorescein-labeled microtubules. Motor concentrations and estimated flux rates are indicated. Left and middle panels compare microtubule depolymerization rates at the same input concentration of motors; left and right panel compare microtubule depolymerization rates at equal motor flux on plus ends. Images were acquired at 15 s intervals.

(E) Depolymerization rates compared at either equal motor input (top) or equal flux on plus ends (bottom). Shown is mean \pm SEM ($n \geq 10$). Microtubules with an initial length of 6–8 μm were chosen for analysis.

displayed an ~30% decrease in run length and an ~60% decrease in the plus end dwell time by comparison with the full-length Kip3 (Figure 3C, Figure S2). These data define a novel role for the Kip3 tail in promoting the binding of Kip3 to microtubule plus ends in vitro.

The Kip3 tail was also required for efficient microtubule depolymerization in vitro. In initial experiments using the same bulk solution concentrations of Kip3 Δ T-LZ and Kip3, the depolymerization of GMPCPP-stabilized microtubules induced by Kip3 Δ T-LZ was lower than that for Kip3 (Figure 3D). However, the run length of Kip3 Δ T-LZ is reduced by 30% in comparison with Kip3. Thus, there is reduced flux of Kip3 Δ T-LZ to the microtubule plus end in these conditions. We measured the motor flux rate by TIRF microscopy and used this input to normalize the protein input in the depolymerase assay. Depolymerization rates were then measured at the same estimated flux of motors (left and right panels in Figure 3D). With this normalization for motility, Kip3 Δ T-LZ still displayed significantly reduced depolymerase activity relative to Kip3 (Figures 3D and 3E). Note that because of the length-dependent depolymerization of microtubules by Kip3, we restricted our analysis of depolymerization rates to microtubules with a starting length of 6–8 μ m (Figure 3E). A similar reduction of depolymerization rates was found upon deletion of the Kip3 tail at all microtubule lengths examined (2–12 μ m, data not shown). This reduction could be, at least partially, due to the decreased dwell time of Kip3 Δ T-LZ on plus ends, because the decreased dwell time will lead to a decrease in the local concentration of the motors on plus ends and a decrease in the time for the motor to remove tubulin subunits before disassociation.

Microtubule Stability Is Sensitive to Change in *KIP3* and *kip3 Δ T-LZ* Dosage

Next, we sought to determine if the approximately 2-fold differences in the depolymerase activity of Kip3 and Kip3 Δ T-LZ were relevant in vivo. First, we compared the fluorescence intensity of Kip3 and Kip3 Δ T-LZ on cytoplasmic microtubule plus ends and found that the accumulation of Kip3 Δ T-LZ on the plus ends is reduced to approximately half of that of Kip3 (Figures 4A and 4B, see arrows). Thus, the Kip3 tail promotes microtubule plus end association to a similar extent both in vivo and in vitro. Because doubling the input of Kip3 Δ T-LZ produces in vitro depolymerase activity comparable to full-length Kip3 (Figure 3E, TOP panel), we next tested whether cells containing two copies of *kip3 Δ T-LZ* would be phenotypically equivalent to cells containing a single copy of wild-type *KIP3* (Figure 4). We created a tandem duplication of *kip3 Δ T-LZ* at the *KIP3* locus, with both *kip3 Δ T-LZ* open reading frames expressed from the *KIP3* promoter (*2xkip3 Δ T-LZ*). We verified that the cells harboring the tandem duplication had an ~2-fold increase in Kip3 Δ T-LZ steady-state protein levels (Figure 4C) and also had an ~2-fold increase in Kip3 Δ T-LZ localized to microtubule plus ends (Figures 4A and 4B). Strikingly, the *2xkip3 Δ T-LZ* cells displayed benomyl sensitivity comparable to *KIP3* cells (Figure 4D). These results suggested that microtubule stability in budding yeast is exquisitely sensitive to Kip3 expression levels. This is indeed the case because a 2-fold increase in wild-type *KIP3* gene dosage results in marked benomyl sensitivity (Figure 4E).

These findings support the conclusion that the magnitude of the observed in vitro defect in depolymerase activity of Kip3 Δ T-LZ is relevant in cells.

The Kip3 Tail Promotes the Binding of Human Kinesin-1 to Microtubule Plus Ends

Next, we determined if the Kip3 tail can promote microtubule plus end binding of a motor that does not concentrate on microtubule plus ends. We generated a chimeric protein that contained the Kip3 tail fused to the C terminus of a tail-less dimeric human kinesin-1 (KHC₅₆₀) (Figures 1A and 3A). Single molecule imaging demonstrated that, relative to the KHC₅₆₀ control, the chimeric motor (hereafter called KHC₅₆₀-CT) had a marked, ~4-fold increase in its dwell time on microtubule plus ends (Figures 5A and 5B and Figure S2). In addition, KHC₅₆₀-CT displayed an increased run length relative to KHC₅₆₀ (Figure 5B). Note that the tail sequence transferred to KHC₅₆₀ does not exactly correspond to the sequences deleted by the Kip3 Δ T-LZ construct: the sequence transferred to KHC₅₆₀ contains an additional 34 amino acid residues from the Kip3 coiled-coil region. This additional sequence helps to maintain the dimeric state of the tail domain (Figure S3).

The Kip3 tail also led to an accumulation of KHC₅₆₀ on microtubule plus ends in vivo. EYFP-tagged KHC₅₆₀ and KHC₅₆₀-CT were expressed from the *KIP3* promoter, replacing the *KIP3* open reading frame. Thus, these strains lack endogenous Kip3, eliminating the possibility of heterodimerization between KHC₅₆₀-CT and Kip3. After confirming that the steady-state protein levels of KHC₅₆₀ and KHC₅₆₀-CT were similar (Figure 5C), we compared the localization of KHC₅₆₀ and KHC₅₆₀-CT on cytoplasmic microtubule plus ends. Although we never observed KHC₅₆₀ concentrated at cytoplasmic microtubule plus ends, KHC₅₆₀-CT accumulated on 34% of astral microtubule plus ends (Figure 5D). Taken together, we conclude that the Kip3 tail is a transferrable domain that can retain kinesin motors on the microtubule plus end.

The Kip3 Tail Has a Stabilizing Effect on Microtubules

Interestingly, the microtubules with KHC₅₆₀-CT enriched at their plus ends were typically long and buckled, indicating that KHC₅₆₀-CT has a stabilizing effect on microtubules (Figure 5D, see asterisks). In support of this conclusion, the average cortical microtubule length was 2.0 ± 0.1 μ m (SEM) in KHC₅₆₀ cells and 4.3 ± 0.2 μ m in KHC₅₆₀-CT cells. Furthermore, astral microtubules with bright KHC₅₆₀-CT signal were on average 7 μ m long, which is never observed in control cells. Thus, when fused to a nondepolymerizing kinesin, kinesin-1, the Kip3 tail, directly or indirectly, enhances the stability of cellular microtubules.

Additionally, we found that the Kip3 tail can inhibit microtubule shrinkage in vitro (Figure 5E). To mimic the shrinking microtubules in vivo, which are mostly composed of GDP-liganded tubulin, we assembled microtubules in the presence of Taxol and GTP. GTP will be quickly hydrolyzed to GDP once microtubules are assembled. After Taxol was further washed out, rapid microtubule shrinkage was induced by adding 100 mM KCl. In the presence of 2 μ M Kip3 tail (purified from *E. coli*, Figure 3A), the microtubule shrinkage rate was decreased by 67%

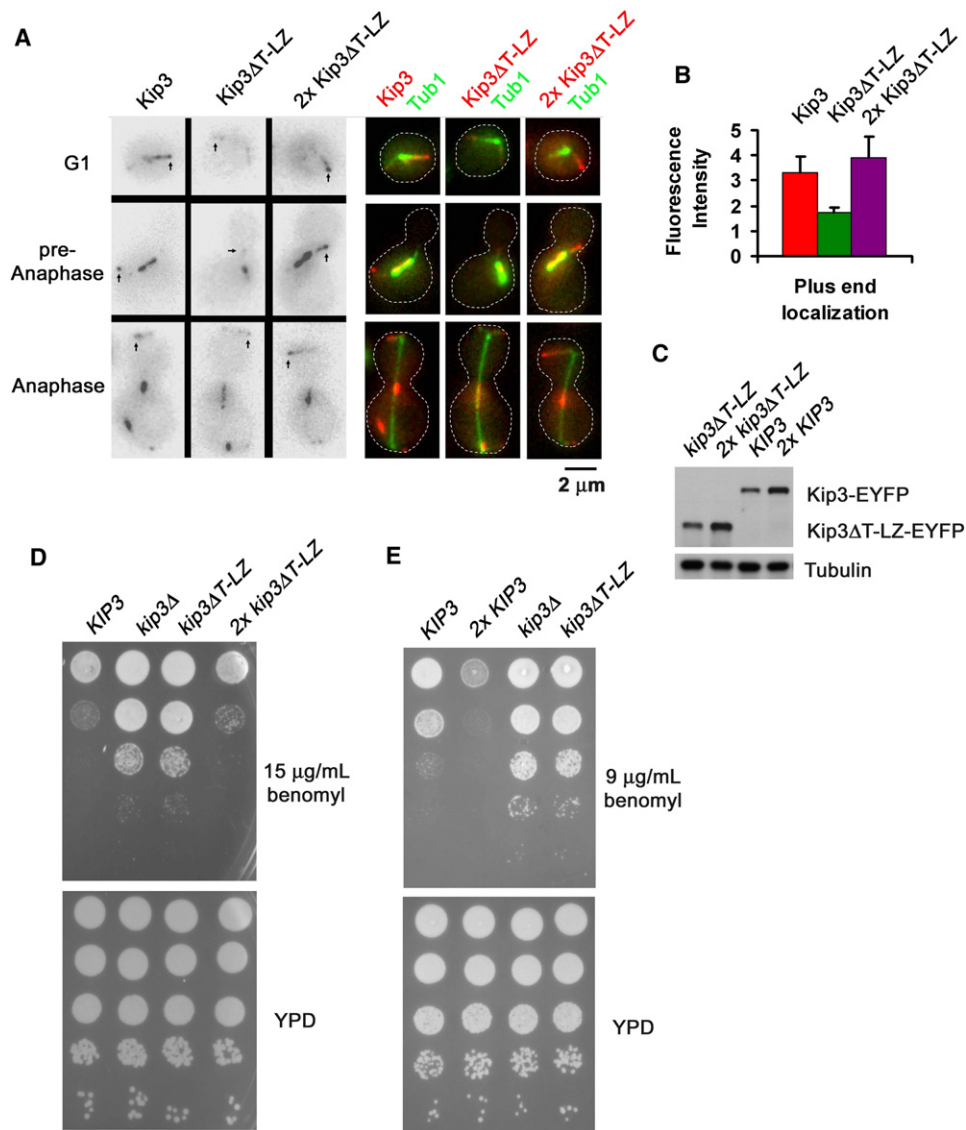


Figure 4. Cellular Microtubule Stability Is Sensitive to KIP3 Dosage

(A) Images of cells expressing one or two copies of Kip3ΔT-LZ-EYFP in strains with one or two copies of *kip3ΔT-LZ* compared to Kip3-EYFP-expressing controls. Microtubules were labeled with CFP-Tub1. Arrows indicate Kip3/Kip3ΔT-LZ on plus ends.

(B) Diminished localization of Kip3ΔT-LZ to cytoplasmic microtubule plus ends in vivo; a 2-fold increase in Kip3ΔT-LZ levels restores microtubule plus end fluorescence intensity to levels comparable with Kip3. N = 43, 57, and 61 for Kip3, Kip3ΔT-LZ, and 2x Kip3ΔT-LZ, respectively. Shown is mean ± SEM.

(C) Steady-state protein levels of Kip3-EYFP and Kip3ΔT-LZ-EYFP in cells that contained one or two copies of the corresponding genes. Shown is a western blot using an anti-GFP antibody. Tubulin serves as a loading control.

(D) Doubling the gene dosage of *kip3ΔT-LZ* results in benomyl sensitivity that is indistinguishable from the wild-type control. The indicated strains were spotted at 10-fold dilutions.

(E) Doubling the gene dosage of *KIP3* results in benomyl hypersensitivity. The indicated strains were spotted at 10-fold dilutions.

(Figure 5E). Thus, the Kip3 tail can stabilize shrinking microtubules in vitro.

Analysis of in vivo microtubule dynamics further supported the hypothesis that the stabilizing effects of Kip3 on shrinking microtubules are mediated by the Kip3 tail. We measured the dynamics of cytoplasmic microtubules in *KIP3*, *kip3ΔT-LZ*, and *kip3Δ* strains. To facilitate visualization of microtubule plus ends, the strains contained Bik1-3YFP, a plus end tracking

protein, in addition to GFP-Tub1, to label microtubule plus ends. Consistent with the notion that the Kip3 tail contributes to the stabilizing effect of Kip3 on microtubules, the shrinkage rates in *kip3ΔT-LZ* strains were higher than in the control strains. In addition, the frequency of rescue is lower in *kip3ΔT-LZ* strains relative to the wild-type control (Table 1). Thus, the Kip3 tail is required for the stabilizing effect of Kip3 on shrinking microtubules.

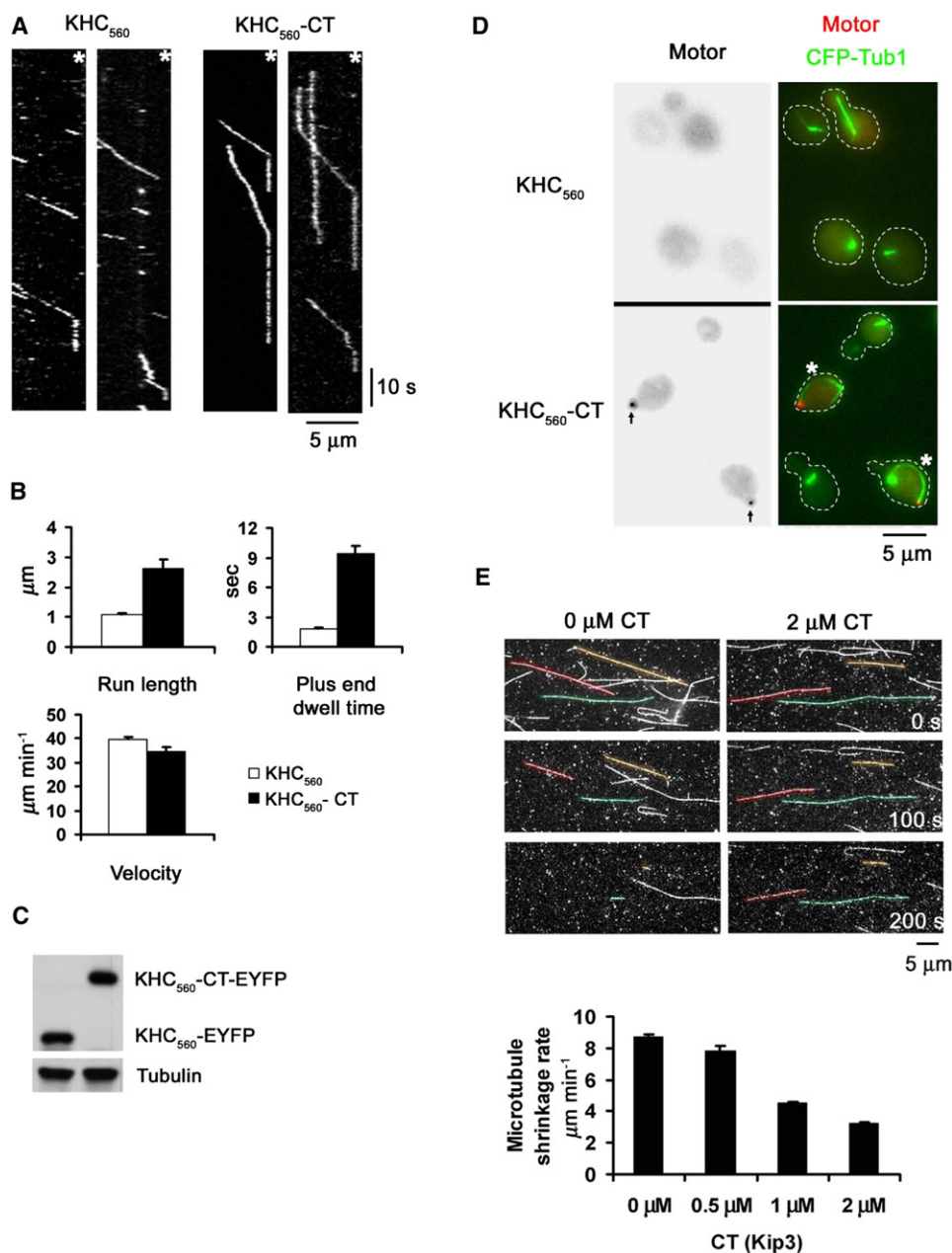


Figure 5. The Kip3 Tail Enables the Binding of Kinesin-1 to Microtubule Plus Ends and Promotes Microtubule Stabilization

(A) Kymographs from TIRF imaging visualizing single KHC₅₆₀ or KHC₅₆₀-CT (KHC-Kip3 tail fusion) molecules walking on Taxol-stabilized microtubules. An image of fluorescein-labeled microtubules was acquired separately to determine the position of microtubule end, as indicated by white asterisks. Note the long dwell time of KHC₅₆₀-CT on microtubule ends, seen as vertical streaks on the kymograph.

(B) The run length, velocity, and plus end dwell time of KHC₅₆₀ and KHC₅₆₀CT. The velocity was fit to a Gaussian curve. The run length and dwell time on plus ends were fit to a first-order exponential curve. Shown is mean ± SEM. Histograms of velocity, run length, and dwell time are shown in Figure S2. Pauses during the translocation of motors were excluded when calculating the velocity.

(C) Comparable steady-state protein levels of KHC₅₆₀-CT and KHC₅₆₀. KHC₅₆₀-CT-EYFP and KHC₅₆₀-EYFP were detected by western blot using anti-GFP antibody.

(D) Enrichment of KHC₅₆₀-CT on astral microtubule plus ends. KHC₅₆₀-EYFP and KHC₅₆₀-CT-EYFP were expressed from the *KIP3* promoter. Microtubules were labeled with CFP-Tub1. Strong enrichment (3-fold over cytoplasmic background) of KHC₅₆₀-CT is observed on 34% of cytoplasmic microtubule plus ends (arrows), whereas enrichment of KHC₅₆₀ was observed on 0% of microtubule plus ends (n = 207). The average cytoplasmic microtubule length was 2.0 ± 0.1 μm (mean ± SEM) in KHC₅₆₀-expressing cells, whereas it was 4.3 ± 0.2 μm in KHC₅₆₀-CT-expressing cells. Asterisks indicate long and buckled microtubules. Cell boundaries are outlined by dashed white line.

(E) The Kip3 tail (CT) inhibits microtubule shrinkage in vitro. (Top) Taxol-stabilized, fluorescein-labeled microtubules were induced to undergo shrinkage by removing Taxol and adding 100 mM KCl with or without the Kip3 tail. Shown are microtubules remaining at selected time points after shrinkage was induced. Individual microtubules are color coded to facilitate visual tracing of shrinkage over time. (Bottom) Quantification of the shrinkage rate. Shown is mean ± SEM (n = 50).

Table 1. Dynamic Instability of Cytoplasmic Microtubules In Vivo

	KIP3	kip3 Δ	kip3 Δ T-LZ
Growth rate ($\mu\text{m min}^{-1}$)	1.3 \pm 0.4	1.2 \pm 0.4	1.3 \pm 0.5
Shrinkage rate ($\mu\text{m min}^{-1}$)	2.6 \pm 0.6*	3.8 \pm 0.8	3.4 \pm 0.7*
Catastrophe frequency (min^{-1})	0.69	0.42	0.51
Rescue frequency (min^{-1})	0.43	0.12	0.13

Twenty-six microtubule life cycles were analyzed for each strain. Rates are reported as mean \pm STD. * $p < 0.0001$ by t test.

The Kip3 Tail Binds Tubulin Dimers and Microtubules

The ability of the Kip3 tail to promote microtubule plus end binding, to enhance the processivity of kinesin motors, and to stabilize microtubules all suggested that this domain might interact with microtubules and possibly tubulin dimers. Using a pelleting assay with Taxol-stabilized microtubules, we found that the Kip3 tail has a weak ($K_d \sim 6 \mu\text{M}$) affinity for microtubules (Figures 6A and 6B). This low affinity is consistent with the Kip3 tail's ability to enhance processivity while still allowing robust directional motility. Moreover, using size exclusion chromatography, we also observed that the Kip3 tail robustly binds tubulin dimers (Figure 6C). The ability of the Kip3 tail to bind tubulin dimers raises the possibility that its activity in promoting plus end binding may involve interactions with surfaces of tubulin that are normally buried within the lattice of the microtubule.

DISCUSSION

The Tubulin-Binding Activity of the Kip3 Tail Explains Its Function in Regulating Microtubule Dynamics

Kinesin-8s are critical regulators of microtubule dynamics, and their importance is underscored by the fact that both human Kif18A and *Drosophila* Klp67A are essential for cell division (Goshima and Vale, 2003; Mayr et al., 2007). Previous work in yeast, *Drosophila*, and human cells suggests that kinesin-8s have complex effects on microtubule dynamics: Kip3, Klp67A, and Kif18A have both destabilizing and stabilizing effects on microtubules (Du et al., 2010; Gatt et al., 2005; Gupta et al., 2006; Stumpff et al., 2008). Our current study defines a novel tubulin-binding activity in the Kip3 tail that has a key role in mediating these complex regulatory effects on microtubule dynamics.

The Kip3 tail robustly binds tubulin dimers, which may be relevant to its ability to promote plus end binding. In common with tubulin dimers, tubulin subunits at the microtubule plus end have more exposed surface than tubulin subunits in the body of the microtubules. Consistent with the idea that tubulin binding mirrors aspects of microtubule plus end binding, the ability to bind tubulin dimers is observed for a number of microtubule plus end-binding proteins (Slep and Vale, 2007). Because of the tubulin dimer-binding activity of the Kip3 tail, it is possible that the tail domain could function as a "latch" that anchors Kip3 to the plus end via direct recognition of unique structural features of the plus end. The transferability of the Kip3 tail to kinesin-1 is consistent with the idea that this domain autonomously binds the plus end. Alternatively, it is equally plausible

that the tail indirectly affects the orientation or conformation of the motor domain at the plus end, facilitating a more robust interaction of the motor domain with the plus end.

The Kip3 tail stabilizes microtubules on its own, which could also be mediated by the tubulin-binding activity. The binding of the Kip3 tail to tubulin (dimers or polymers) could alter the conformation of tubulin subunits at the microtubule plus end, perhaps favoring a straighter conformation and more stable organization of tubulin subunits at the end. Alternatively but not exclusively, the Kip3 tail could stabilize microtubules by cross-linking adjacent tubulin subunits. This is possible, since the dimeric tail can bundle microtubules (Figure S4), which suggests each tail dimer has at least two tubulin-binding sites.

Does the Kip3 tail promote an interaction of Kip3 with the plus end that is different from the effect of the Kip3 tail when Kip3 is walking along the lattice? The estimated k_{off} of Kip3 and Kip3 Δ T-LZ is consistent with the conclusion that the tail could promote a specific interaction of Kip3 with the plus end. Based on the measurements of run lengths and velocities, the k_{off} for Kip3 from the lattice is 0.38 min^{-1} , whereas the k_{off} for Kip3 Δ T-LZ is 0.55 min^{-1} . From the dwell time data, the k_{off} for Kip3 from the plus end is 1.61 min^{-1} , whereas the k_{off} for Kip3 Δ T-LZ is 3.68 min^{-1} . Thus, the tail has an $\sim 60\%$ greater effect on the motor's dissociation from the plus end relative to its effect on dissociation from the lattice. A similar, but even greater, effect of the Kip3 tail is observed in the context of the fusion to kinesin-1. As discussed above, this differential effect could be explained if the Kip3 tail interacts with the surfaces of tubulin that are available at the microtubule end but not along the lattice.

Integrating Kip3's Regulation of Microtubule Dynamics with Cellular Microtubule Length Control

What determines whether Kip3 destabilizes or stabilizes microtubules? Kip3 destabilizes microtubules during the growing phase, whereas it stabilizes microtubules during the shrinkage phase. We previously reported that Kip3 is highly enriched on growing microtubules, whereas there is no detectable accumulation of Kip3 on shrinking microtubules (Gupta et al., 2006). This suggests the possibility that the concentration of Kip3 on plus ends affects the effect of Kip3 on microtubule dynamics. Indeed, Kip3 was reported to depolymerize the GTP-cap-mimic-stabilized microtubules in a cooperative manner (Varga et al., 2009).

Our findings suggest a model in which the concentration of Kip3 on the plus ends determines whether Kip3 destabilizes or stabilizes microtubules (Figure 7). We propose that when microtubules grow, Kip3 lands on the lattice and walks toward the plus end. Because the velocity of Kip3 is typically faster than the growth rate of microtubules (Gupta et al., 2006; Varga et al., 2006), Kip3 accumulates on the plus ends. The accumulation is facilitated by the Kip3 tail, which helps to retain Kip3 on the plus ends. At these high local concentrations of Kip3, cooperative interactions among motors occur, the motor triggers catastrophe, and the microtubule starts to shrink. Although the large accumulation of Kip3 is lost from the plus ends, Kip3 motors continue to walk to the shrinking plus end. At these lower concentrations of Kip3, the tail domain-dependent stabilizing

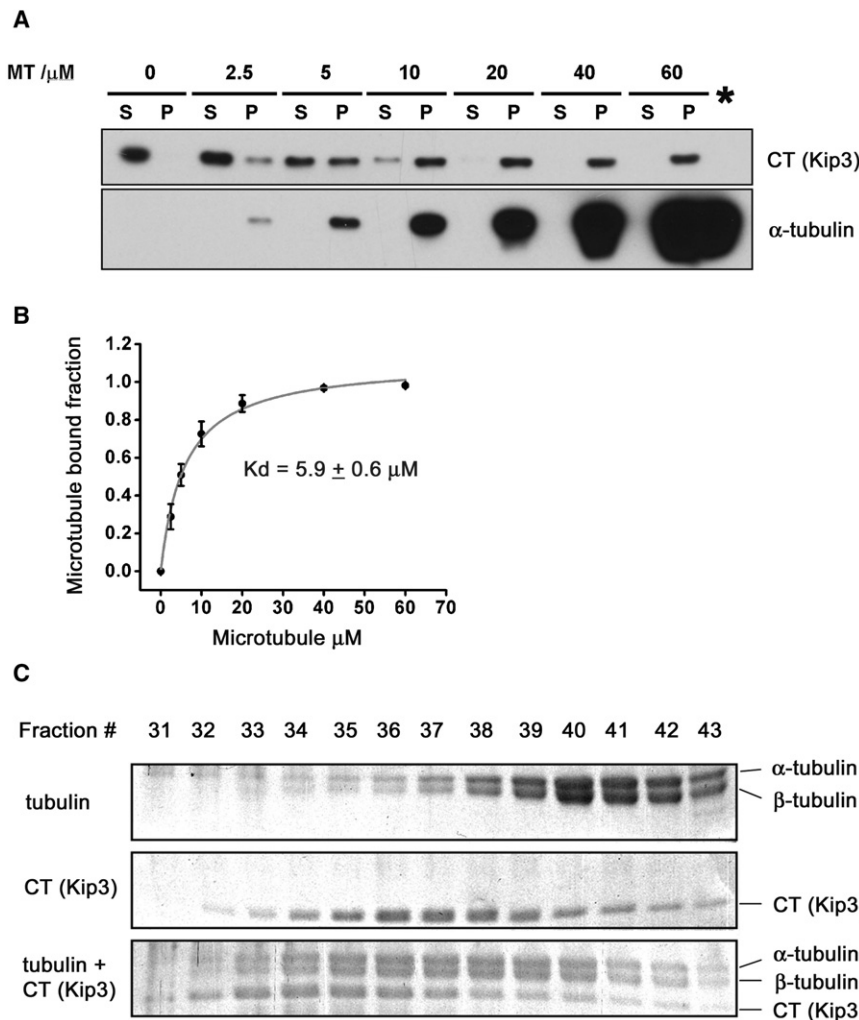


Figure 6. The Kip3 Tail Binds Microtubules and Tubulin Dimers

(A) Copelleting of the Kip3 tail with taxol-stabilized microtubules. Input, 2.5 μ M Kip3 tail. Western blotting was used to detect the Kip3 tail and tubulin because the bands of Kip3 tail and tubulin overlapped on Coomassie-stained gels after SDS-PAGE when the tubulin input was over 10 μ M. (Asterisk) Input of microtubules only, showing that the antibody recognizing Kip3 tail did not cross-react with tubulin.

(B) Graph of the percentage of Kip3 tail bound plotted against the concentration of polymerized tubulin. Fitting of the data to a one-site saturation-binding model gave a dissociation constant (K_d) of $5.9 \pm 0.6 \mu\text{M}$. Each data point is presented as mean \pm SEM ($n = 3$).

(C) A protein complex between the Kip3 tail and tubulin. Size exclusion chromatography of tubulin (top), CT (Kip3) (middle), and CT (Kip3) + tubulin (bottom). Column fractions were analyzed by Coomassie staining after SDS-PAGE. Input, 2.5 μ M Kip3 tail, 2 μ M tubulin. Fraction volume, 0.325 mL. Fractionation of molecular weight standards for this experiment are as follows (molecular weight [kD] / fraction number / V_e [mL]): 670/26/8.2; 158/35/11.3; 44/45/14.3; and 17/49/15.9.

effects of Kip3 dominate, with the net effect of slowing the shrinkage rate and increasing the rescue frequency. Thus, we propose that Kip3 has concentration-dependent stabilizing and destabilizing effects: individual motors at low concentrations at the plus end exert a stabilizing effect, but at high concentrations groups of motors destabilize the microtubule. Although our model defines direct effects of Kip3 in regulating microtubule dynamics, we do not exclude the additional possibility that Kip3 could exert indirect effects via changing the stoichiometry of other +TIPs.

It is interesting to consider one apparent exception to this model. During late anaphase, when the spindle disassembles, Kip3 actually increases the shrinkage rate of the shrinking microtubules of the two half-spindles (Woodruff et al., 2010). However, unlike shrinking cytoplasmic microtubules, we find that Kip3 is highly enriched on the plus end of shrinking spindle microtubules at the end of anaphase (data not shown). The mechanism for recruiting Kip3 onto shrinking spindle microtubules during anaphase is not known but presumably involves specific Kip3 interactions with spindle midzone proteins. Thus, this apparent exception is actually consistent with our model: a high concen-

tration of Kip3 on the plus end destabilizes the microtubule, whereas low concentrations promote stability.

Our findings also add to the notion that Kip3 has a key role in maintaining a narrow distribution of cellular microtubule lengths, and thus matches microtubule lengths to their cellular functions. The discovery of the remarkable processivity of Kip3 led to the proposal that Kip3's dest-

stabilizing activity is length dependent (Varga et al., 2009): long microtubules have more Kip3 on the plus end and a higher probability of catastrophe, because long microtubules collect more Kip3 molecules that all walk to the plus end. The net effect would be to narrow the distribution of microtubule lengths in cells by destabilizing longer microtubules. The stabilizing effect of Kip3 that becomes evident at low Kip3 concentrations would further accentuate this effect by stabilizing shorter microtubules.

The Function of Kinesin-8's Tail May Be Conserved

Is the plus end-targeting function of the Kip3 tail a general property of kinesin-8s, or does it reflect a budding yeast-specific adaptation? There are reasons to favor the former idea that the tail domains of kinesin-8s share conserved functions. Most significantly, contemporaneous work from other groups has uncovered the fact that the tail domain of the human kinesin-8, Kif18A, binds microtubules and promotes the plus end accumulation of Kif18A (P. Ohi and C. Walczak, personal communication). This could reflect convergent evolution or reflect underlying structural homology. Intriguingly, although the tail domains of kinesin-8s show no detectable similarity by conventional methods,

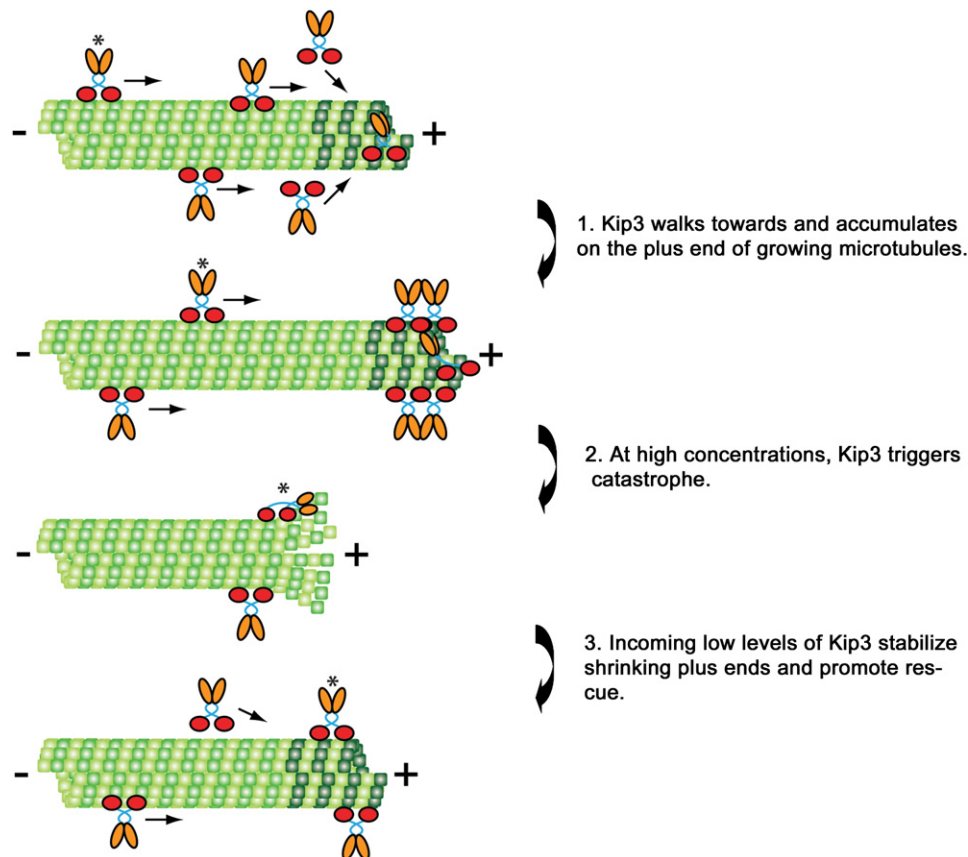


Figure 7. A Model for Dual-Mode Regulation of Microtubule Dynamics by Kip3

(1) When microtubules grow, Kip3 walks toward and accumulates on the plus end, which is facilitated by the Kip3 tail. (2) At high concentrations, Kip3 triggers microtubule catastrophe. Microtubules then shrink and the bulk of Kip3 molecules are lost from the plus end. (3) Other Kip3 molecules reach the shrinking plus end. At the lower concentrations of Kip3, the stabilizing effects dominate, slowing the shrinkage rate and increasing the rescue frequency, in a manner that requires the Kip3 tail. Note that Kip3 could be affected by or cooperate with other +TIPs to regulate microtubule dynamics, which is not depicted in this model. Asterisks indicate the history of the same motor.

we identified conserved peptide motifs in the tail domains of all kinesin-8s using MEME (Bailey et al., 2009). We found at least four such motifs (Figure S5) that collectively identify kinesin-8 family members in a MAST (Bailey et al., 2009) query of the NCBI nonredundant protein database, including Kif19s, which were not used to define the motifs. Only at very high E values ($E > 1$) do we start detecting a small number of kinesins from other families. The presence of these motifs thus raises the possibility that the tails might have similar structural features, and it is consistent with their apparent functional similarity.

Dosage-Sensitive Regulators of Genome Stability in Tumor Development

Our findings raise a final interesting issue. We found that yeast cells are exquisitely sensitive to *KIP3* gene dosage. This reinforces the notion that Kip3 is a central nodal point for the cellular regulation of microtubule dynamics. Additionally, the identification of dosage sensitivity for microtubule function or other aspects of genome stability has implications for understanding the phenotypic consequences of aneuploidy. Aneuploidy, although producing only small-scale changes in gene expres-

sion, could create a storm of additional genetic instability through effects on critical dosage-sensitive regulators such as *KIP3* (Duesberg et al., 2006). The end result could be more rapid acquisition of novel cellular characteristics.

EXPERIMENTAL PROCEDURES

Strains

Table S1 provides a list of yeast and bacterial strains used in this manuscript. Yeast strains were in the S288C background (isogenic to BY4742) except those used for protein overexpression and purification, which were in the W303-1A background. The details of strain construction and other information are available upon request.

Constructs and Protein Purification

The coding sequence for the N-terminal Halo (Promega)-tagged full-length Kip3 (1–805), Kip3 Δ T (1–480), Kip3 Δ T –LZ (with residues 250–281 from Gcn4) and C-terminal Halo-tagged human KHC₅₆₀ (1–560), KHC₅₆₀-CT (Kip3 447–805) were expressed from the *GAL1* promoter on 2 μ plasmids (pRS425 backbone). A protease-deficient yeast strain was used for protein expression (Hovland et al., 1989). Protein expression was induced by addition of 2% galactose for 18 hr prior to harvesting cells. Ni²⁺ affinity chromatography and ion exchange chromatography were used for protein purification. See the

Supplemental Information for detailed description. Protein concentration was determined by Bradford assay. The concentration of dimers is reported in all figures except Figures S1 and S3.

The Kip3 tail (CT, Kip3 aa 447–805), with an N-terminal GST tag and a C-terminal 6His tag, was expressed in *E. coli* BL21 cells. Protein expression was induced with 0.2 mM IPTG at 37°C for 4 hr. Cells were lysed and proteins purified by glutathione Sepharose 4B (GE Healthcare) chromatography. The Kip3 tail was cleaved by TEV protease treatment at room temperature for 2.5 hr.

Motility Assays

Assay chambers with a volume of about 10 μ l were made by forming a “coverslip-double-sided tape-glass slide” sandwich. The chambers were sequentially coated with 1 mg/mL biotin-BSA and 0.5 mg/mL streptavidin, allowing Taxol-stabilized microtubules to be immobilized on the coverslips (see the Supplemental Experimental Procedures for stabilized microtubule preparation). For Kip3, the reaction mixtures contained BRB80 buffer at pH 7.2 supplemented with 0.5 mg/mL casein, 5% glycerol, 2 mM ATP-Mg, 20 μ M Taxol, 100 mM KCl, and oxygen scavenging mix (0.2 mg/mL glucose oxidase, 0.035 mg/mL catalase, 25 mM glucose, and 70 mM β -mercaptoethanol). For KHC, the reaction mixture contained 50 mM HEPES at pH 7.4, 0.5 mg/mL casein, 5% glycerol, 2 mM ATP-Mg, 20 μ M Taxol, and oxygen scavenging mix. Images were recorded every 2 s for 20 min (Kip3) or every 0.5 s for 5 min (KHC) using an Olympus IX-81 TIRF microscope.

Depolymerase Assay

Experimental conditions were similar to those for the motility assay, with the following modifications: GMPCPP-stabilized microtubules were used instead of Taxol-stabilized microtubules. Taxol was not included in the reaction mixtures. Wide-field images were acquired every 15 s for 12.5 min using a Zeiss AXIO Imager M1 microscope.

Microtubule Stability Assay

The assay chambers were prepared as for the motility assay. Taxol-stabilized microtubules were first diluted in a 1:60 ratio into BRB80 (no Taxol) before being carried by flow into the chamber. After 20 min incubation, chambers were washed with BRB80. Microtubule shrinkage was induced by flowing BRB80 containing 100 mM KCl and oxygen scavenging mix. Images were recorded every 5 s for 5 min.

Size Exclusion Chromatography and Pelleting Assay

For the size exclusion chromatography, 2.5 μ M Kip3 tail (CT) and 2 μ M tubulin were incubated at 4°C for 30 min in column buffer (BRB80, 50 mM NaCl, 1 mM DTT at pH 6.8) and then loaded onto a 0.32 \times 30 cm Superdex-200 FPLC column (Bio-Rad). For the pelleting assay, the Kip3 tail preparation was pre-spun at 80,000 rpm (Sorvall RP100AT3) for 5 min and then incubated with Taxol-stabilized microtubules in the column buffer (above) with 20 μ M Taxol at room temperature for 15 min, prior to centrifugation at 80,000 rpm for 5 min. Tubulin and the Kip3 tail were detected with a mouse anti- α -tubulin (DM1 α , Sigma) and rabbit anti-polyhistidine (Cell Signaling) antibody, respectively.

Cellular Imaging

Most strains were grown to log phase in SC media prior to imaging. The exception was for KHC₅₆₀- and KHC₅₆₀-CT-expressing strains, where cells were directly taken from fresh plates. To determine the intensity of Kip3-EYFP and Kip3 Δ T-LZ-EYFP at microtubule plus ends, a Z series image stack was collected and the fluorescence intensity was measured from a maximal intensity projection. Cellular background was subtracted for quantification. To measure relative amounts of EYFP-labeled motors in the nucleus and the cytoplasm, Kip3-EYFP- or Kip3 Δ T-LZ-EYFP-expressing cells were treated with 35 μ g/mL nocodazole for 15 min followed by fixation with 4% paraformaldehyde fixation for 10 min and then stained with 1 μ g/mL DAPI for 5 min. The plane containing the brightest signal of the CFP-Tub1-marked spindle pole body was selected for analysis. To measure microtubule dynamics, a Z focal plane series of images (seven planes with 0.75 μ m between adjacent planes) was acquired at 6 s intervals, enabling a three-dimensional measurement of microtubule length.

Petri Plate Assays

To compare benomyl sensitivity of the strains, cells were grown in liquid YPD culture at 30°C for 1 day and then spotted onto YPD plates containing benomyl in a 1:10 series dilution. Plates were placed at 24°C for 2 days and then photographed.

SUPPLEMENTAL INFORMATION

Supplemental Information includes five figures, one table, Supplemental Experimental Procedures, and Supplemental References and can be found with this article online at [doi:10.1016/j.molcel.2011.06.027](https://doi.org/10.1016/j.molcel.2011.06.027).

ACKNOWLEDGMENTS

We thank T. Mitchison, R. King, S. Gilbert, C. Moores, J. Al-Bassam, M. Betterton, M. Kwon, N. Ganem, S. Godinho, and K. Knouse for discussions and comments on the work. D.P. was supported by Howard Hughes Medical Institute and a National Institutes of Health grant (GM61345). J.B.P.-L. received support from the HMS/Portugal Program in Translational Research.

Received: April 20, 2011

Revised: June 18, 2011

Accepted: June 21, 2011

Published: September 1, 2011

REFERENCES

- Akhmanova, A., and Steinmetz, M.O. (2008). Tracking the ends: a dynamic protein network controls the fate of microtubule tips. *Nat. Rev. Mol. Cell Biol.* 9, 309–322.
- Bailey, T.L., Boden, M., Buske, F.A., Frith, M., Grant, C.E., Clementi, L., Ren, J., Li, W.W., and Noble, W.S. (2009). MEME SUITE: tools for motif discovery and searching. *Nucleic Acids Res.* 37, W202–W208.
- Carvalho, P., Timauer, J.S., and Pellman, D. (2003). Surfing on microtubule ends. *Trends Cell Biol.* 13, 229–237.
- Desai, A., and Mitchison, T.J. (1997). Microtubule polymerization dynamics. *Annu. Rev. Cell Dev. Biol.* 13, 83–117.
- DeZwaan, T.M., Ellingson, E., Pellman, D., and Roof, D.M. (1997). Kinesin-related KIP3 of *Saccharomyces cerevisiae* is required for a distinct step in nuclear migration. *J. Cell Biol.* 138, 1023–1040.
- Du, Y., English, C.A., and Ohi, R. (2010). The kinesin-8 Kif18A dampens microtubule plus-end dynamics. *Curr. Biol.* 20, 374–380.
- Duesberg, P., Li, R., Fabarius, A., and Hehlmann, R. (2006). Aneuploidy and cancer: from correlation to causation. *Contrib. Microbiol.* 13, 16–44.
- Gaijart, N. (2010). Plus-end-tracking proteins and their interactions at microtubule ends. *Curr. Biol.* 20, R528–R537.
- Gandhi, R., Bonaccorsi, S., Wentworth, D., Doxsey, S., Gatti, M., and Pereira, A. (2004). The *Drosophila* kinesin-like protein KLP67A is essential for mitotic and male meiotic spindle assembly. *Mol. Biol. Cell* 15, 121–131.
- Gardner, M.K., Odde, D.J., and Bloom, K. (2008). Kinesin-8 molecular motors: putting the brakes on chromosome oscillations. *Trends Cell Biol.* 18, 307–310.
- Gatt, M.K., Savoian, M.S., Riparbelli, M.G., Massarelli, C., Callaini, G., and Glover, D.M. (2005). Klp67A destabilises pre-anaphase microtubules but subsequently is required to stabilise the central spindle. *J. Cell Sci.* 118, 2671–2682.
- Goshima, G., and Vale, R.D. (2003). The roles of microtubule-based motor proteins in mitosis: comprehensive RNAi analysis in the *Drosophila* S2 cell line. *J. Cell Biol.* 162, 1003–1016.
- Gouveia, S.M., and Akhmanova, A. (2010). Cell and molecular biology of microtubule plus end tracking proteins: end binding proteins and their partners. *Int. Rev. Cell Mol. Biol.* 285, 1–74.
- Grissom, P.M., Fiedler, T., Grishchuk, E.L., Nicastro, D., West, R.R., and McIntosh, J.R. (2009). Kinesin-8 from fission yeast: a heterodimeric, plus-end-directed motor that can couple microtubule depolymerization to cargo movement. *Mol. Biol. Cell* 20, 963–972.

- Gupta, M.L., Jr., Carvalho, P., Roof, D.M., and Pellman, D. (2006). Plus end-specific depolymerase activity of Kip3, a kinesin-8 protein, explains its role in positioning the yeast mitotic spindle. *Nat. Cell Biol.* 8, 913–923.
- Hovland, P., Flick, J., Johnston, M., and Sclafani, R.A. (1989). Galactose as a gratuitous inducer of GAL gene expression in yeasts growing on glucose. *Gene* 83, 57–64.
- Howard, J., and Hyman, A.A. (2009). Growth, fluctuation and switching at microtubule plus ends. *Nat. Rev. Mol. Cell Biol.* 10, 569–574.
- Mayr, M.I., Hummer, S., Bormann, J., Gruner, T., Adio, S., Woehlke, G., and Mayer, T.U. (2007). The human kinesin Kif18A is a motile microtubule depolymerase essential for chromosome congression. *Curr. Biol.* 17, 488–498.
- Mitchison, T., and Kirschner, M. (1984). Dynamic instability of microtubule growth. *Nature* 312, 237–242.
- Nakai, K., and Horton, P. (1999). PSORT: a program for detecting sorting signals in proteins and predicting their subcellular localization. *Trends Biochem. Sci.* 24, 34–36.
- Poulain, F.E., and Sobel, A. (2010). The microtubule network and neuronal morphogenesis: dynamic and coordinated orchestration through multiple players. *Mol. Cell. Neurosci.* 43, 15–32.
- Schroer, T.A. (2001). Microtubules don and doff their caps: dynamic attachments at plus and minus ends. *Curr. Opin. Cell Biol.* 13, 92–96.
- Schuyler, S.C., and Pellman, D. (2001). Microtubule “plus-end-tracking proteins”: the end is just the beginning. *Cell* 105, 421–424.
- Slep, K.C., and Vale, R.D. (2007). Structural basis of microtubule plus end tracking by XMAP215, CLIP-170, and EB1. *Mol. Cell* 27, 976–991.
- Straight, A.F., Sedat, J.W., and Murray, A.W. (1998). Time-lapse microscopy reveals unique roles for kinesins during anaphase in budding yeast. *J. Cell Biol.* 143, 687–694.
- Stumpff, J., von Dassow, G., Wagenbach, M., Asbury, C., and Wordeman, L. (2008). The kinesin-8 motor Kif18A suppresses kinetochore movements to control mitotic chromosome alignment. *Dev. Cell* 14, 252–262.
- Tischer, C., Brunner, D., and Dogterom, M. (2009). Force- and kinesin-8-dependent effects in the spatial regulation of fission yeast microtubule dynamics. *Mol. Syst. Biol.* 5, 250. 10.1038/msb.2009.5.
- Varga, V., Helenius, J., Tanaka, K., Hyman, A.A., Tanaka, T.U., and Howard, J. (2006). Yeast kinesin-8 depolymerizes microtubules in a length-dependent manner. *Nat. Cell Biol.* 8, 957–962.
- Varga, V., Leduc, C., Bormuth, V., Diez, S., and Howard, J. (2009). Kinesin-8 motors act cooperatively to mediate length-dependent microtubule depolymerization. *Cell* 138, 1174–1183.
- Walczak, C.E., and Heald, R. (2008). Mechanisms of mitotic spindle assembly and function. *Int. Rev. Cytol.* 265, 111–158.
- Wargacki, M.M., Tay, J.C., Muller, E.G., Asbury, C.L., and Davis, T.N. (2010). Kip3, the yeast kinesin-8, is required for clustering of kinetochores at metaphase. *Cell Cycle* 9, 2581–2588.
- Wehrle-Haller, B., and Imhof, B.A. (2003). Actin, microtubules and focal adhesion dynamics during cell migration. *Int. J. Biochem. Cell Biol.* 35, 39–50.
- West, R.R., Malmstrom, T., Troxell, C.L., and McIntosh, J.R. (2001). Two related kinesins, klp5+ and klp6+, foster microtubule disassembly and are required for meiosis in fission yeast. *Mol. Biol. Cell* 12, 3919–3932.
- West, R.R., Malmstrom, T., and McIntosh, J.R. (2002). Kinesins klp5(+) and klp6(+) are required for normal chromosome movement in mitosis. *J. Cell Sci.* 115, 931–940.
- Wickstead, B., and Gull, K. (2006). A “holistic” kinesin phylogeny reveals new kinesin families and predicts protein functions. *Mol. Biol. Cell* 17, 1734–1743.
- Woodruff, J.B., Drubin, D.G., and Barnes, G. (2010). Mitotic spindle disassembly occurs via distinct subprocesses driven by the anaphase-promoting complex, Aurora B kinase, and kinesin-8. *J. Cell Biol.* 191, 795–808.